Penetration of the Signal Sequence of *Escherichia coli* PhoE Protein into Phospholipid Model Membranes Leads to Lipid-Specific Changes in Signal Peptide Structure and Alterations of Lipid Organization†

A. M. Batenburg,‡ R. A. Demel,‡ A. J. Verkleij,§ and B. de Kruijff*,‖

Department of Biochemistry, Department of Molecular Cell Biology, and Institute of Molecular Biology and Medical Biotechnology, State University of Utrecht, Padualaan 8, 3584 CH Utrecht, The Netherlands

Received September 28, 1987; Revised Manuscript Received February 3, 1988

ABSTRACT: In order to obtain more insight in the initial steps of the process of protein translocation across membranes, biophysical investigations were undertaken on the lipid specificity and structural consequences of penetration of the PhoE signal peptide into lipid model membranes and on the conformation of the signal peptide adopted upon interaction with the lipids. When the monolayer technique and differential scanning calorimetry are used, a stronger penetration is observed for negatively charged lipids, significantly influenced by the physical state of the lipid but not by temperature or acyl chain unsaturation as such. Although the interaction is principally electrostatic, as indicated also by the strong penetration of N-terminal fragments into negatively charged lipid monolayers, the effect of ionic strength suggests an additional hydrophobic component. Most interestingly with regard to the mechanism of protein translocation, the molecular area of the peptide in the monolayer also shows lipid specificity: the area in the presence of PC is consistent with a looped helical orientation, whereas in the presence of cardiolipin a time-dependent conformational change is observed, most likely leading from a looped to a stretched orientation with the N-terminus directed toward the water. This is in line also with the determined peptide–lipid stoichiometry. Preliminary ^{31}P NMR and electron microscopy data on the interaction with lipid bilayer systems indicate loss of bilayer structure.

The development of the signal hypothesis (Blobel & Dobberstein, 1975) triggered extensive biochemical and genetic research in the field of secretion and membrane incorporation of proteins. N-terminal extensions, the signal or leader sequences, were found obligatory and satisfactory for membrane translocation, and proteinaceous factors have been identified (Walter & Blobel, 1980; Meyer et al., 1982) which in the eukaryotic system target the protein to the endoplasmic reticulum membrane through which translocation must occur; in prokaryotes, a similar machinery may function, involving the products of the sec genes (Oliver & Beckwith, 1981; Shiba et al., 1984) and soluble factors (Müller & Blobel, 1984). Yet the question of how the secretory proteins, large and hydrophilic molecules, are able to pass the barrier formed by the membrane remains unanswered. In principle, two opposing ideas have been proposed. One postulates a porteinaceous translocator machinery (Steiner et al., 1980; Blobel, 1980; Singer et al., 1987); in the other, a passage through the lipid part of the membrane is suggested (Di Rienzo et al., 1978; von Heijne & Blomberg, 1979; Engelmann & Steitz, 1981), initiated by interaction of the signal peptide with the lipids. These signal sequences are characterized by a hydrophilic, basic N-terminal region, followed by a stretch of apolar, mainly hydrophobic, residues (Perlman & Halvorson, 1983; von Heijne, 1984). In analogy with peptides of comparable amphiphilicity (Bougis et al., 1983; Habermann, 1972), this structure seems to be ideally fit for interaction with lipids, rather than for interaction with proteins, which usually requires a more stringent primary structure homology. Moreover, interaction of precursors with amphiphiles, brought about by their signal sequence region, was reported (Nanba et al., 1984; Dierstein & Wickner, 1985), and translocation of precursors was demonstrated into phospholipid vesicles in which only bacterial leader peptidase was reconstituted (Ohno Iwashita & Wickner, 1983) and even into pure lipidvesicles (Geller & Wickner, 1985), strongly supporting the idea of lipid involvement. Also, isolated, chemically synthesized signal peptides were found to interact with lipid model membranes (Shinnar & Kaiser, 1984), resulting in insertion into the hydrophobic core of the bilayer (Nagaraj, 1984). The correlation shown for the LamB mutated signal sequences between in vivo functioning, α-helix formation, and ability to penetrate into phospholipid monomolecular films (Briggs et al., 1985) is in favor of a functional role of protein–lipid interactions in the translocation process. It should be realized, however, that additional factors like the membrane potential and soluble or membrane-bound proteinaceous components [see, for instance, Wiech et al. (1987) and Wiedman et al. (1987) for the eukaryotic case] most likely play a direct or indirect role in the translocation process.

Among the arguments raised against a lipidic translocation pathway, the unfavorable energetics of passage of the polar protein through the hydrophobic acyl chain region are often mentioned (Singer et al., 1987). Physicochemical studies, however, have shown that, although most phospholipids under physiological conditions are organized in bilayers, alternative structures can also be adopted, as reviewed in de Kruijff et al. (1985). Especially in model systems containing negatively charged phospholipids, inverted nonbilayer lipid structures can be induced by interaction with certain basic and amphiphilic, hence signal sequence resembling, polypeptides (Batenburg,

† These studies were carried out under the auspices of the Netherlands Foundation for Chemical Research (SON) and with financial aid from the Netherlands Organization for Scientific Research (NWO).

* Address correspondence to this author.
‡ Department of Biochemistry.
§ Department of Molecular Cell Biology.
‖ Institute of Molecular Biology and Medical Biotechnology.

0006-2960/88/0427-5678$01.50/0

et al., 1985, 1987a), and, as was suggested earlier by several authors (Nesmeyanova, 1982; de Kruijff et al., 1981; Sjöström et al., 1987), the inverted lipid structures are attractive candidates to form a hydrophilic transport pathway for the polar portions of the newly synthesized protein, worthy of a further investigation.

In an earlier study (Batenburg et al., 1988), we characterized the interfacial behavior of the chemically synthesized signal sequence of the *Escherichia coli* outer membrane pore protein PhoE. This signal sequence is essential for translocation of the protein across the *E. coli* cytoplasmic membrane (de Vrije et al., 1987). In accordance with earlier findings on other signal peptides (Rosenblatt et al., 1980; Briggs & Gierasch, 1984; Laxma Reddy & Nagaraj, 1985), an induction of largely α-helical structure was demonstrated in a hydrophobic or amphiphilic environment, and the experimental results, combined with conformation predictions, suggested a looped type of organization in monolayers of the highly surface-active peptide. Here, we report on the interaction of the signal peptide with lipid model systems. The monomolecular layer technique is used to investigate the lipid specificity of the insertion of the peptide, the molecular area of the peptide, and the kinetics of the penetration process. The effect of the signal peptide on the thermotropic behavior of the lipid was studied with differential scanning calorimetry, and, in light of the above-mentioned speculations, the possible influence of the peptide on the lipid macroscopic organization was investigated with ^{31}P NMR and freeze–fracture electron microscopy. The results witness a strong preference for negatively charged phospholipids, a lipid- and time-dependent reorganization of the peptide, and suggest the induction of lipid nonbilayer structures.

Materials and Methods

Materials. Peptides were synthesized by solid-phase synthesis as reported before (Batenburg et al., 1988). The sodium salt of bovine heart cardiolipin was obtained according to published purification procedures (Smaal et al., 1985), during which bovine heart phosphatidylserine (PS)[1] was recovered as a side product. *E. coli* phospholipids were isolated by Bligh and Dyer extraction (Bligh & Dyer, 1959) of cells in the late log phase and purified by column chromatography with Polygosil (63–100 μm, Macherey-Nagel) as stationary phase and chloroform/methanol 50:50 (v/v) as eluent, after a first elution of neutral lipids and other contaminants with 100% chloroform. *E. coli* PE was isolated from this total phospholipid extract by separation on preparative thin-layer chromatography plates (Merck, 11845) run with chloroform/methanol/water 75:25:2.5 (v/v) and Polygosil column chromatography with chloroform/methanol/25% ammonia/water 68:28:2:2 (v/v). Soybean PC and egg PC were isolated according to standard procedure, and PC species were synthesized as described before (van Deenen & de Haas, 1964). Egg PG and DMPS were prepared by phospholipase D catalyzed transesterification of egg PC and DMPC in the presence of glycerol or serine, respectively (Comfurius & Zwaal, 1977). The purity of all lipids was confirmed by thin-layer chromatography.

Anhydrous sodium cyanoborohydride was purchased from Aldrich and was used within 1 month after delivery; 10 Ci/mol [^{14}C]formaldehyde (NEC 039H) was from NEN. All other chemicals were of analytical grade or better.

^{14}C Labeling of PhoE Signal Peptide. The reductive methylation of the α- and ϵ-amino groups of the signal peptide, a labeling procedure that leaves the charge intact, was based on the procedure of Dottavio-Martin and Ravel (1978). In view of the insolubility of the peptide in water, however, both labeling and isolation of the product were performed in trifluoroethanol. Shortly, 3 mg of peptide was dissolved as described below in 160 μL of trifluoroethanol, the pH was adjusted to 8 with *N*-methylmorpholine, and 25 μCi of [^{14}C]-formaldehyde (2.5 μmol/20 μL) and 20 μL of 6 mg/mL $NaCNBH_3$, both dissolved in water, were successively added. After a 25-h incubation at ambient temperature, the labeled peptide was separated from unbound label on a 15 × 0.5 cm Sephadex LH20 column run with trifluoroethanol; the radioactivity of 5 μL of the 80-μL fractions was determined with scintillation counting. The peptide eluted after 1.8 mL, well resolved from the low molecular weight side products at 2.7 mL. The obtained labeling was usually around 5000 dpm/nmol, which implies that, on the average, one out of every five molecules had obtained one methylated amino group.

Sample Preparation and Standard Procedures. Phospholipid dispersions were prepared by hydration of a dry lipid film. The peptides were dissolved in a small amount of trifluoroacetic acid (approximately 10 μL/mg), dried with a nitrogen stream, and finally dissolved in trifluoroethanol, at concentrations between 1 and 10 mg/mL. Under vortexing, the peptide was added to lipid dispersions in such a way that the final concentration of trifluoroethanol was maximally 2% (5% for the NMR experiment with the highest peptide:lipid ratio); if necessary, the pH was readjusted, and the samples were concentrated by a 30-min 27000*g* centrifugation. The absence of lipid degradation was checked after sample preparation. For CD, a 10 mM phosphate buffer, pH 7.3, was used; for monolayer experiments, a buffer containing 10 mM PIPES, 100 mM NaCl, and 1 mM EDTA, pH 7.3 (unless otherwise stated) was used; and for all other measurements, 25 mM PIPES, 100 mM NaCl, and 1 mM EDTA, pH 7.3, were used; if not otherwise indicated, the experiments were performed at 25 °C. Exact peptide stock concentrations were determined by quantitative amino acid analysis with asparagine as an external standard, after 48 h of 5.8 N HCl hydrolysis in sealed vacuum tubes; an LKB 4151 Alpha Plus amino acid analyzer was used. Phospholipid was determined as inorganic phosphate, after destruction with perchloric acid (Fiske & Subbarow, 1925; Rouser et al., 1975).

Monolayer Experiments. Monolayer surface tension was measured by the (platinum) Wilhelmy plate method, using an LM 500 microbalance, and surface radioactivity was determined with a Betron LB 203E equipped with a Berthold LB 6280 gas flow counter. The counter was placed right above the monolayer, where it only monitors the radioactive material inserted in the monolayer, since radiation from the subphase is efficiency quenched. Constant area experiments were performed with a 20-mL Teflon trough with a 5.5 × 5.5 cm surface. For measurements at constant pressure, a 5 × 15 cm Teflon trough with a movable barrier was used containing 60 mL of subphase. Starting with a 5 × 5 cm area, the position of the barrier was adjusted by an ABU11 autoburette, controlled by a TTT2 titrator (both from Radiometer, Copenhagen), which was connected with the microbalance; at the other side of the barrier, a 40 mN/m dipalmitoyl-PC monolayer was spread to avoid surface absorption of the peptide. Phospholipids were spread on the surface and peptide injected from a 1 mg/mL trifluoroethanol solution in the subphase with

[1] Abbreviations: PC, phosphatidylcholine; PE, phosphatidylethanolamine; PG, phosphatidylglycerol; PIPES, 1,4-piperazinediethanesulfonic acid; PS, phosphatidylserine; DEPS, dielaidoyl-PS; DMPC, dimyristoyl-PC; DMPG, dimyristoyl-PG; DMPS, dimyristoyl-PS; DOPS, dioleoyl-PS; DSC, differential scanning calorimetry.

Hamilton syringes. Monolayers were collected with about 90% efficiency by aspiration through a glass capillary directly into a scintillation vial, while manually decreasing the monolayer area with a movable barrier; the radioactivity of an equal volume of subphase was always subtracted. For pressure–area curves, a 17.2 × 33.2 cm Teflon trough was used; here, the monolayer was compressed with a speed of 1 cm/min by a moving barrier. The buffer used for all monolayer experiments was prepared from water, triply distilled in an all-glass apparatus, and the surface was carefully cleaned before lipid spreading.

Other Physical Studies. ^{31}P NMR was carried out at 121.5 MHz with a Bruker MSL 300, while applying broad-band proton decoupling as reported earlier (Chupin et al., 1987). The procedures for small-angle X-ray scattering and freeze–fracture electron microscopy were also described earlier (Batenburg et al., 1987a). For DSC, a Perkin-Elmer DSC 4 was used with a scan rate of 2 °C/min; further details are given elsewhere (Batenburg et al., 1987a); afterward, the exact amount of lipid present in the pans was determined after dissolving the contents in methanol/chloroform 1:1 (v/v).

Results

Constant Area Monolayer Experiments. The primary structure of the synthesized peptide corresponding to the 21-residue signal sequence of the PhoE protein is Met-Lys-Lys-Ser-Thr-Leu-Ala-Leu-Val-Val-Met-Gly-Ile-Val-Ala-Ser-Ala-Ser-Val-Gln-Ala. The peptide is poorly soluble in aqueous solvents, and upon introduction from trifluoroethanol in water under a clean interface, peptide monolayers are spontaneously formed to a maximal surface pressure of 25 mN/m (Batenburg et al., 1988). Similarly, interaction of the peptide with lipid monolayers could be followed by measurement of the surface pressure increase in a constant area setup. Since extrinsic proteins and other nonpenetrative agents do not induce an increase of monolayer surface pressure (Demel et al., 1973), this effect can be related to the degree and nature of penetration. The highest initial pressure allowing penetration, the critical insertion pressure, is often used as a measure of the penetrative force. To investigate the lipid specificity of this insertion process, experiments were performed with the zwitterionic soybean PC and the negatively charged bovine heart cardiolipin, membrane phospholipids with a similar acyl chain composition, rich in linoleic acid (Batenburg et al., 1987b). As shown in Figure 1A, the maximal pressure increase in both lipids is dependent on the peptide concentration in the subphase up to 0.15 μM, but at all concentrations, the penetration in the cardiolipin monolayer proceeds up to much higher pressures. It should be mentioned that no pressure change was observable when only the solvent was injected. For further experiments, an injected amount of 10 nmol of peptide was chosen, apparently amply sufficient to saturate the monolayer and to produce a stable end pressure within 15 min. Figure 1B shows that the preference of the basic peptide for the negatively charged lipid is expressed in an approximately 12 mN/m difference between the final pressures, independent of the initial pressure. Increasing the temperature has virtually no effect on the pressure increase in either of these two lipids. As is clear from Figure 1B, a comparable lipid specificity is observed for the chemically synthesized signal sequence of the M13 coat protein (amino acid sequence Met-Lys-Lys-Ser-Leu-Val-Lys-Ala-Ser-Val-Ala-Val-Ala-Thr-Leu-Val-Pro-Met-Leu-Ser-Phe-Ala; Wickner, 1979). PC here shows a somewhat larger pressure increase, but this should be related to the higher equilibrium pressure of 29.5 mN/m of the pure peptide monolayer obtainable by absorption from the subphase

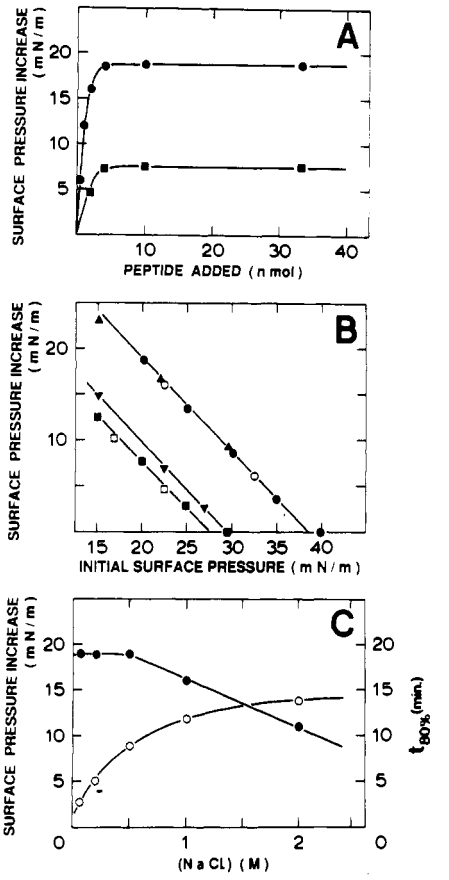

FIGURE 1: Surface pressure increase of monolayers of PC and cardiolipin as a function of (A) the amount of signal peptide injected in the subphase, (B) the initial pressure, and (C) the ionic strength. Signal peptide was injected from a 1 mg/mL trifluoroethanol solution into 20 mL of subphase. (A) PhoE signal peptide induced pressure increase in (●) a cardiolipin monolayer and (■) a soy PC monolayer at 22 °C. (B) As in (A), open symbols are at 37 °C; M13 coat signal peptide induced pressure increase in cardiolipin (▲) and soy PC (▼) at 22 °C. (C) PhoE signal peptide induced final pressure increase in cardiolipin (●) and time required to obtain 80% of that final increase (○). In (A) and (C), an initial pressure of 20 mN/m was applied; in (B) and (C), 10 nmol of peptide was injected.

(not shown). For the cardiolipin monolayer, however, a remarkably similar final pressure was attained upon insertion of both peptides.

The stronger interaction of the PhoE signal peptide with negatively charged lipid is indicative of an interaction based on an electrostatic attraction. In contrast to other basic polypeptides such as apocytochrome *c* (Pilon et al., 1987), however, a relatively high salt concentration is needed to affect the final pressure attained in cardiolipin (Figure 1C), suggesting an additional strong hydrophobic contribution to the interaction; at salt concentrations lower than 0.5 M, only the rate of pressure increase is influenced. The surface pressure of monolayers of bovine heart PS, another highly unsaturated (Rietveld et al., 1986) negatively charged phospholipid, can be increased by penetration of PhoE signal peptide up to similarly high values (Figure 2). With PS molecular species, the influence of lipid physical state and unsaturation was studied. It can be seen that in liquid-crystalline DMPS a similar pressure increase is achieved as in the unsaturated natural PS and the less unsaturated DOPS and DEPS; yet, at 18 °C, where at pressures higher than 20 mN/m DMPS is known to form a condensed, gel-state monolayer (Demel et al., 1987), penetration is limited to much lower pressures. Thus, physical state, but not unsaturation as such, determines the maximal surface pressure in charged monolayers.

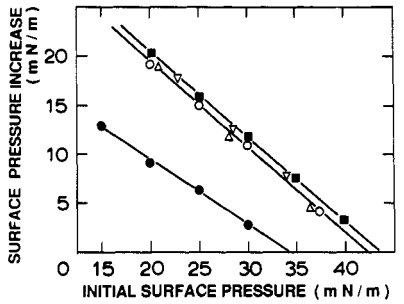

FIGURE 2: Effect of lipid acyl chain unsaturation and physical state on the signal peptide induced surface pressure increase in PS monolayers. (■) Bovine heart PS, 22 °C; (●) DMPS, 18 °C; (○) DMPS, 30 °C; (△) DEPS, 30 °C; (▽) DOPS, 30 °C; 10 nmol of PhoE signal peptide was injected.

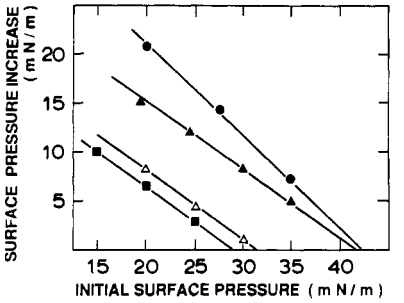

FIGURE 3: Signal peptide induced surface pressure increase in monolayers of *E. coli* total phospholipid extract and its two major lipid classes. (▲) *E. coli* extract at 37 °C and (△) *E. coli* extract at 22 °C; (■) *E. coli* PE at 37 °C and (●) egg PG at 37 °C; 10 nmol of PhoE signal sequence was added.

The phospholipid fraction of *E. coli* membranes is composed of 75% PE, 20% PG, and 5% cardiolipin (Burnell et al., 1980). In order to see if the PhoE signal peptide would also be able to penetrate into the lipid part of its putative target membrane, the total phospholipid extract and its two major components were also included in our study. PG exhibited similar behavior as the other negatively charged phospholipids, while the surface pressure increase in PE is comparable with that in PC (Figure 3). In the total phospholipid extract, however, in spite of the relatively small amount of negatively charged lipids, penetration continues to much higher pressures, and the critical insertion pressure, the maximal pressure allowing penetration, is even close to that in the pure PG. Interestingly, in this lipid mixture, lowering the temperature does decrease the maximal pressure; this could suggest a difference in physical state, for which, however, no proof could be derived from pressure–area characteristics and DSC (not shown). The pressures attained at 22 °C are in the same range as reported for the LamB signal peptide in PE/PG monolayers (Briggs et al., 1985).

PhoE signal peptide fragments I (Met^1–Ala^7), I–II (Met^1–Gly^{12}), and III (Ile^{13}–Ala^{21}), roughly corresponding with the hydrophilic, basic N region, with this region plus the hydrophobic central region and with the C region, respectively (von Heijne, 1985), were also studied for their ability to penetrate monolayers of zwitterionic and negatively charged lipids. Not surprisingly, fragment III, lacking a net charge, shows weak penetration and no specificity, while the basic fragments I and I–II, like the complete sequence, penetrate much stronger into cardiolipin monolayers (Figure 4). The critical pressures of the latter two for insertion in cardiolipin are distinctly higher than for the whole signal peptide, which is especially remarkable for fragment I since it does not show any surface activity on itself (Batenburg et al., 1988). Unlike the behavior of the total sequence, the maximally attainable pressure is highly dependent on the initial pressure.

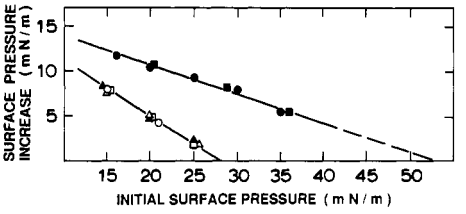

FIGURE 4: Monolayer surface pressure increase induced by PhoE signal sequence fragments. Closed symbols are for cardiolipin and open symbols for soy PC monolayers. (●, ○) Fragment I (Met^1–Ala^7), (■, □) fragment I–II (Met^1–Gly^{12}), and (▲, △) fragment III (Ile^{13}–Ala^{21}). Circa 20 nmol was injected.

Molecular Area and Kinetics of Monolayer Penetration. The radiolabeled signal peptide was able to produce a pressure increase in cardiolipin monolayers, similar to the unlabeled peptide. More important, injection of a 1:1 mixture of labeled and unlabeled peptide led to incorporation of about 50% of the radioactivity that was absorbed after injection of labeled peptide only. Hence, it was concluded that the radiolabeled signal peptide behaved similar to the parent molecule.

For determination of the signal peptide's molecular area, two types of experiments were performed. First, constant area experiments were used; via the pressure–area curve of the lipid, which was very similar for soy PC and cardiolipin, the measured pressure increase resulting from peptide penetration can be translated into the area occupied by the peptide, assuming a neglectable condensing effect. Three nanomoles of peptide at an initial pressure of 20 mN/m for cardiolipin and, for better accuracy, 15 mN/m for PC was used. From the results, combined with the determination of the amount of absorbed radioactivity and knowledge of the peptide's specific activity, the molecular area was calculated. In cardiolipin, a peptide area was thus established of 165 ± 15 Å^2 (mean and standard deviation of 10 measurements with 2 different batches of radioactive peptide); in soy PC, on the other hand, a much larger value of 345 ± 40 Å^2 was found. In the second approach, the area increase at constant pressure was measured, directly leading to the peptide molecular area. Here an equilibrium situation is studied, the pressure being kept at a value of 30 mN/m, close to the equivalence membrane pressure (Demel et al., 1975), and the effect observed is determined by the interaction equilibrium and is not limited by the developed pressure. Hence, once the occupied area is known, one can also obtain information about the affinity and stoichiometry of the interaction by analyzing the area increase as a function of the amount of peptide injected in the subphase. Figure 5A shows two representative results for penetration in cardiolipin; an injected amount of 10 nmol of labeled peptide was used for molecular area determinations. With these experiments, an area per peptide molecule was determined of 180 ± 50 Å^2 (n = 5), the relatively large error being due to variations in area increase rather than in absorbed radioactivity, yet the result being in line with that of the more accurate constant area experiments.

Injection of 30 nmol of peptides under a cardiolipin monolayer of 30 mN/m leads to an approximately 95% area increase (Figure 5A), and further additions of peptide do not result in a further increase, indicating that the lipid is saturated with peptide. A similar conclusion can be drawn from Figure 5B. On the basis of this maximal increase, a peptide molecular area of 165 Å^2, and a cardiolipin molecular area of 120 Å^2 (Shah et al., 1965), a peptide–lipid phosphate stoichiometry can be calculated of 1:2.8 ± 0.4 mol/mol. With an iterative nonlinear regression program based on the equation $K_D = [L_N][P][PL_N]^{-1}$ (in which K_D = the dissociation constant, P

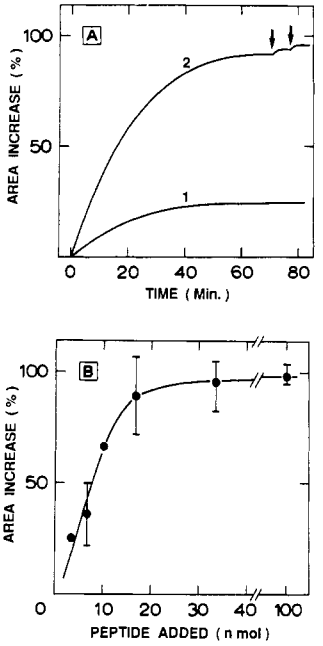

FIGURE 5: Monolayer area increase resulting from PhoE signal peptide penetration at constant pressure. (A) Kinetics of the area increase for (1) 7 nmol and (2) 30 nmol of injected peptide. The arrows indicate extra additions of 30 nmol of peptide. (B) Final area increase measured 2 h after addition as a function of the amount of injected peptide; where possible, the range of the results is indicated. Surface pressure, 30 mN/m; subphase volume, 60 mL.

= the free peptide, and L_N and PL_N are the free and occupied peptide binding sites, respectively) (Hille et al., 1981), a K_D of 0.10 ± 0.01 μM was calculated from this "binding curve". Though the formula does not include a full description of the complex process of surface absorption, the results can be used for comparative purposes (Batenburg et al., 1985, 1987a; Pilon et al., 1987). If, for a fixed amount of peptide, the concentration of free peptide is directly determined on the basis of the subphase radioactivity instead of deduced from the total amount injected, a comparable K_D = 0.12 μM is found by application of the same equation. The values should be considered as a maximum though, since part of the "free" peptide may be present in an aggregated form (Batenburg et al., 1988), resulting in an underestimation of the actual affinity.

The kinetics of the monolayer insertion were followed in a constant area setup by continuous measurement of the surface radioactivity; for a better sensitivity, a low initial surface pressure of 10 mN/m was used to allow more peptide to be incorporated. The final surface radioactivity and thus the amount of penetrated peptide are much higher in cardiolipin than in PC, with an only slightly larger area occupancy of the peptide (Figure 6), confirming the difference between the molecular areas reported above. Contrasting the simple kinetics of insertion in the zwitterionic lipid, the pressure increase in cardiolipin follows two-phase kinetics. This was observed earlier in the experiments of the preceding paragraph, where the reported data apply to the final pressures. Similar two-phase kinetics were found for the other negatively charged lipids for all peptide concentrations and all initial pressures studied and appeared to be specific for the complete signal sequence. The observation of this behavior also in cases where initial pressures much higher than 25 mN/m (collapse pressure of the pure peptide monolayer; Batenburg et al., 1988) were applied excludes the formation of patches of peptide monolayer as the process underlying the first phase. It is the second phase that is affected by the ionic strength of the subphase in the way described in the first paragraph under Results. Both

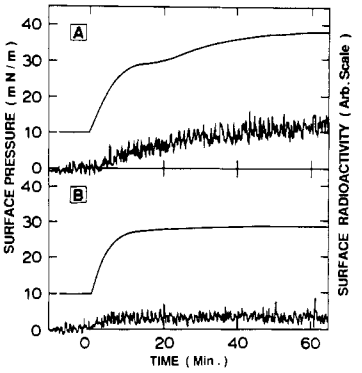

FIGURE 6: Kinetics of the increase of surface pressure (upper trace) and surface radioactivity (lower trace) upon injection of ^{14}C-labeled PhoE signal peptide. (A) Cardiolipin monolayer; (B) soy PC monolayer; 6 nmol of peptide was injected.

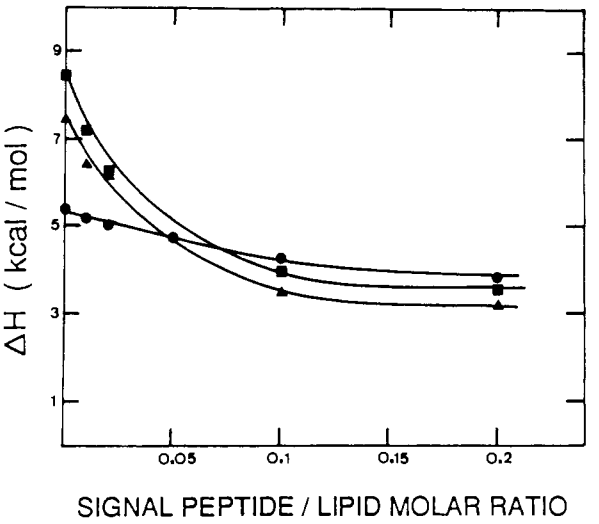

FIGURE 7: Enthalpy of the phospholipid main phase transition as a function of the applied PhoE signal peptide:lipid molar ratio: (●) DMPC; (▲) DMPG, (■) DMPS.

phases appear to be accompanied by an increase of radioactivity in the monolayer (Figure 6); interestingly, the second phase, characterized by an only 35% increase of peptide occupied area, leads to a radioactivity increase of circa 150%. Knowing the final molecular area to be 165 Å^2 (see above), the peptide molecular area after the first phase can be estimated to be approximately 300 Å^2; thus, in the second phase, a continued penetration appears to be accompanied by a change in molecular area.

Differential Scanning Calorimetry. In order to study the consequences of signal peptide–lipid interactions in bilayer systems, DSC experiments were carried out for which DMPC, DMPS, and DMPG were chosen on the basis of their favorable phase transitions. With DSC, the phase transitions of the lipid acyl chains can be monitored. Decrease of the enthalpy of the cooperative transition is due to disturbance of the acyl chain packing, in particular in the gel state. The transition temperatures and enthalpies measured for the pure lipids were in good agreement with earlier reports (van Dijck et al., 1976; Rietveld et al., 1985; Mombers et al., 1979). The DMPC pretransition at 12 °C disappears upon peptide addition, an effect already accomplished at the lowest peptide:lipid ratio studied. The peak corresponding to the main transition is broadened, but its enthalpy content is only slightly reduced upon peptide addition (Figure 7), without a major change in transition temperature. For the two negatively charged lipids, the effect on the enthalpy content is much larger, and the shift to lower temperature is also somewhat more pronounced,

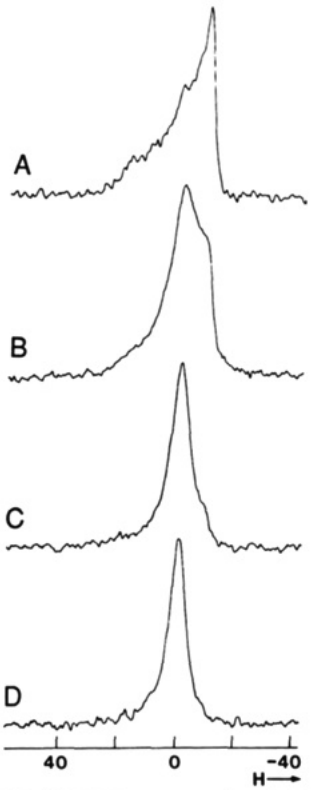

FIGURE 8: 121.5-MHz ^{31}P NMR spectra of cardiolipin in the presence of PhoE signal peptide. (A) Pure lipid. Peptide:P_i molar ratio 1:30 (B), 1:10 (C), and 1:3 (D).

especially for DMPS (approximately 5 °C at a lipid:protein ratio of 10, versus 1.5 °C for PC). The enthalpy decrease is nonlinear (Figure 7); the reduced influence at higher peptide:lipid ratios is not necessarily due to clustering of the peptide in the membrane but can equally well be caused by the aggregation of the peptide in the aqueous phase (Batenburg et al., 1988) which makes it unable to interact with the lipid; initially, 1 peptide molecule prevents circa 15 negatively charged lipid molecules from participating in the cooperative transition. The DSC scans were completely reproducible upon rescanning.

Analysis of Lipid Structural Changes. To get a first insight into the influence of the PhoE signal peptide on the macroscopic organization of phospholipids, cardiolipin was chosen, which shows a well-documented isothermal polymorphism modulated by divalent cations as well as basic peptides (de Kruijff et al., 1985; Batenburg et al., 1985, 1987a). Addition of the peptide from trifluoroethanol solution to lipid dispersions results at peptide:lipid molar ratios above 1:20 (on P_i base) in immediate and complete precipitation of the lipid in large aggregates. The shape of the phosphorus NMR spectrum can be used to gain insight into the lipids' freedom of reorientation and hence their macroscopic organization (Seelig, 1978). The ^{31}P NMR spectrum of the pure cardiolipin is composed of a high-field peak and low-field shoulder (Figure 8), such as usually found for lipids in bilayers of low curvature, the fast long-axis rotation of the molecules leading to partial averaging of the chemical shift anisotropy. The presence of increasing amounts of peptide is correlated with the rise of an isotropic spectral component. Since the lipid was readily pelleted, the isotropic signal should not be related to small structures but reflects diffusion along structures of high curvature within the macroscopically large complexes. At a molar ratio of 1:10 on P_i base, the "bilayer" type of signal has almost disappeared, and the isotropic spectrum shows no further changes up to a ratio of 1:3, at which point, according to the monolayer data, saturation is attained.

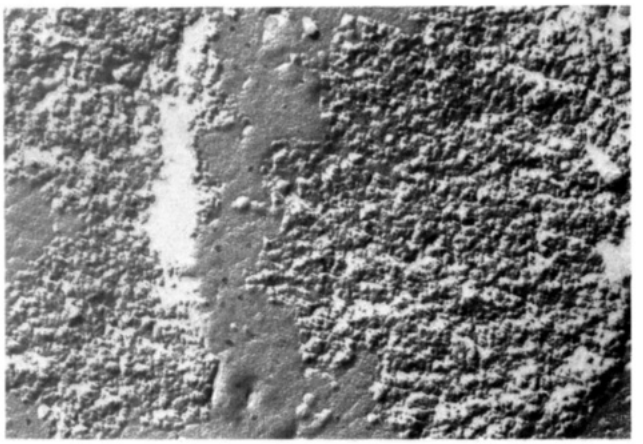

FIGURE 9: Freeze–fracture electron microscopy of a PhoE signal peptide–cardiolipin complex of peptide:P_i molar ratio 1:3. Final magnification 55000×.

To get a better characterization of the structure underlying the isotropic NMR signal, small-angle X-ray scattering and electron microscopy were used. X-ray measurements in the same range of peptide:lipid ratios gave little information, showing a broad scatter maximum around 60 Å but no sharp reflections, indicating the absence of regular subunit stacking in the complexes (not shown). Electron microscopy of pure cardiolipin dispersions (not shown) visualizes spherical smooth bilayers. Freeze–fracture of samples of peptide:lipid molar ratio 1:30 and 1:10 reveals a rather heterogeneous picture yet indicates a gradual disappearance of bilayer structure. At a ratio of 1:3, the highest peptide:lipid ratio studied, no lamellar structure is seen anymore, and the replicas show large aggregates of indistinctly ordered granules (Figure 9).

Discussion

The mechanism of protein translocation across the bacterial inner membrane is largely unknown, yet the signal (or leader) peptide appears to be essential, and several lines of evidence (Ohno Iwashita & Wickner, 1983; Briggs et al., 1985; Yatvin, 1987) suggest a role for the membrane phospholipids. This study describes various biophysical aspects of signal peptide–phospholipid interactions.

The lipid preference for penetration of signal peptides into model membranes was studied with the monolayer technique. Since agents interacting solely with the lipid headgroups without penetration into the monolayer were shown not to affect the area or surface pressure of monolayers (Demel et al., 1973), changes in these parameters are usually assumed to reflect directly the partitioning of solutes into the monolayer. PhoE signal sequence induced pressure increase appears to be much larger in negatively charged lipids and is dependent on the lipid physical state but not on the degree of lipid acyl chain unsaturation; the signal peptide of the M13 coat protein exhibited a similar lipid specificity. The pressure increases are more pronounced than observed for most of the cardiotoxins (Bougis et al., 1981), for (apo)-cytochrome *c* (Pilon et al., 1987), and for the presequence of mitochondrial cytochrome oxidase subunit IV (Tamm, 1987), and comparable with that for melittin (Bougis et al., 1981). The preference for charged lipids indicates an important electrostatic component of the interaction, which is underlined by the high penetrative capacity of the small N-terminal fragment I, not containing a long hydrophobic sequence and most likely inserted between the lipid headgroups.

The relatively low "limiting pressure" for insertion into zwitterionic lipids, hardly exceeding the equilibrium spreading pressure of the pure peptide, suggests an absolute requirement for negatively charged lipids for incorporation into a natural membrane, for which an "equivalence pressure" of 25–35 mN/m has been estimated (Demel et al., 1975; Schindler, 1979). On the other hand, it is shown that the additional presence of small (25%) amounts of charged lipids already results in a marked stimulation of penetration, especially at higher pressures, as was shown earlier for a mitochondrial presequence (Tamm, 1987). DSC results are also in favor of a specific insertion of the peptide into membranes of negatively charged phospholipids.

A large portion of our measurements was concerned with the conformation of the PhoE signal peptide in the lipid monolayer, especially with its occupied area. In a cardiolipin monolayer, constant area and constant pressure experiments using ^{14}C-labeled peptide indicated a similar peptide molecular area; from the more accurate constant area data, a value of 165 Å^2 was calculated. This value is consistent with an α-helical conformation perpendicular to the plane of the monolayer (Batenburg et al., 1988); 75% α-helix structure was indeed shown for the peptide in SDS micelles (Batenburg et al., 1988), and preliminary circular dichroism measurements pointed to α-helix formation also in the presence of negatively charged phospholipid membranes. Interestingly, in PC, a much larger area of 345 Å^2 was determined, very close to what was established for the peptide area in a pure PhoE signal peptide monolayer (360 Å^2; Batenburg et al., 1988), interpreted, in combination with computerized predictions of conformation, as in favor of a looped structure of the peptide with both the N- and the C-terminus in the water phase. A parallel alignment of the helix, such as deduced for mitochondrial presequences (Tamm, 1987), would have resulted in a still larger area.

Most important, the kinetics of the monolayer insertion, studied with the use of continuous surface radioactivity measurements, pointed to a time-dependent conformational change of the peptide in the presence of negatively charged phospholipids, involving a decrease of the occupied area from 300 to 165 Å^2; the 300 Å^2 should be considered as a minimum, since part of the molecules may already have reoriented at this stage. The most straightforward explanation in our view is as follows. First, the peptide inserts as a looped helix, involving a nick around the glycine residue, a helix breaker often found in signal peptides. This conformation is conserved in PC (at low surface pressure) and is the stable situation in the pure peptide monolayer. In the neighborhood of negatively charged lipid, however, a second and apparently rate-limiting step takes place in which the C-terminus is moved away from the lipid–water interface. The resulting stretched orientation will allow full interaction between the three positive charges at the N-terminus and the negative lipid headgroups, without the interference of the bulky, negatively charged C-terminus. An electrostatic basis of this process is in agreement with the retardation of the reorientation at high ionic strength; the observation of two-phase kinetics also in situations of small amounts of incorporated peptide makes a peptide–peptide interaction as a driving force highly unlikely. Interestingly such a conformational change would shuttle the site of attachment of the mature sequence across the membrane and is an important element of the "loop-model" for protein translocation (Inouye & Halegoua, 1980). Direct topological information, especially with respect to the C-terminus, will be needed, however, to establish the exact nature of the conformational change and to prove its validity in bilayer systems; preliminary results of experiments based on the labeling of amino groups in the cardiolipin monolayer by fluorescamine were consistent with a position of the N-terminus close to the aqueous phase. The signal peptide–cardiolipin stoichiometry is also in favor of the proposed (final) orientation with the positive charge cluster being exactly counterbalanced by three negative lipid charges.

A last subject of study was the possible modulation of lipid organization by the signal peptide. ^{31}P NMR showed for cardiolipin a peptide:lipid ratio dependent induction of a broad isotropic signal superimposed on the original "bilayer" spectrum, indicative of high internal curvature in the large structures formed. Since the complexes under the studied conditions do not form ordered arrays, electron microscopy is the most informative of the techniques used. At the expense of bilayer organization, patches of granular structure are formed, closely resembling the morphology encountered for cardiolipin saturated with cardiotoxin II, which on the basis of additional evidence was interpreted as reflecting inverted lipid structures (Batenburg et al., 1985). These preliminary observations of structural changes induced by signal peptide reinforce the speculations of nonbilayer lipid involvement in the translocation process (Nesmeyanova, 1982; de Kruijff et al., 1985; Sjöström et al., 1987); direct evidence for a functional role, however, remains to be obtained.

Added in Proof

Using *E. coli* mutants defective in the biosynthesis of negatively charged phospholipids, an involvement of PG in the translocation of the precursor of PhoE across the inner membrane could be directly demonstrated (de Vrije et al., 1988).

Acknowledgments

We thank P. Vermeij for the DSC work and J. Leunissen-Bijvelt for the freeze–fracturing. T. de Vrije is kindly acknowledged for the purification of *E. coli* total phospholipid extract and *E. coli* PE and Dr. W. Wickner (UCLA) for his gift of M13 coat signal peptide.

Registry No. DEPS, 63976-14-7; DMPC, 18194-24-6; DMPG, 61361-72-6; DMPS, 64023-32-1; DOPS, 70614-14-1.

References

Batenburg, A. M., Bougis, P. E., Rochat, H., Verkleij, A. J., & de Kruijff, B. (1985) *Biochemistry 24*, 7101–7110.

Batenburg, A. M., Hibbeln, J. C. L., Verkleij, A. J., & de Kruijff, B. (1987a) *Biochim. Biophys. Acta 903*, 142–154.

Batenburg, A. M., Hibbeln, J. C. L., & de Kruijff, B. (1987b) *Biochim. Biophys. Acta 903*, 155–165.

Batenburg, A. M., Brasseur, R., Ruysschaert, J.-M., Van Scharrenburg, G. J. M., Slotboom, A. J., Demel, R. A., & De Kruijff, B. (1988) *J. Biol. Chem. 263*, 4202–4207.

Bligh, E. G., & Dyer, W. J. (1959) *Can. J. Biochem. Physiol. 37*, 911–913.

Blobel, G. (1980) *Proc. Natl. Acad. Sci. U.S.A. 77*, 1496–1500.

Blobel, G., & Dobberstein, B. (1975) *J. Cell Biol. 67*, 852–862.

Bougis, P. E., Rochat, H., Pieroni, G., & Verger, R. (1981) *Biochemistry 20*, 4915–4920.

Bougis, P. E., Tessier, M., van Rietschoten, J., Rochat, H., Faucon, J.-F., & Dufourcq, J. (1983) *Mol. Cell. Biochem. 55*, 49–64.

Briggs, M., S. & Gierasch, L. M. (1984) *Biochemistry 23*, 3111–3114.

Briggs, M. S., Gierasch, L. M., Zlotnick, A., Lear, J. D., & De Grado, W. F. (1985) *Science (Washington, D.C.) 228*, 1096–1099.

Burnell, E., van Alphen, L., Verkleij, A. J., & de Kruijff, B. (1980) *Biochim. Biophys. Acta 597*, 492–501.
Chupin, V., Killian, J. A., & de Kruijff, B. (1987) *Biophys. J. 51*, 395–405.
Comfurius, P., & Zwaal, R. F. A. (1977) *Biochim. Biophys. Acta 488*, 36–42.
de Kruijff, B., Verkleij, A. J., van Echteld, C. J. A., Gerritsen, W. J., Noordam, P. C., Mombers, C., Rietveld, A., de Gier, J., Cullis, P. R., Hope, M. J., & Nayar, R. (1981) in *International Cell Biology 1980–1981* (Schweiger, H. G., Ed.) pp 559–571, Springer, Berlin.
de Kruijff, B., Cullis, P. R., Verkleij, A. J., Hope, M. J., van Echteld, C. J. A., & Taraschi, T. F. (1985) in *The Enzymes of Biological Membranes* (Martonosi, A., Ed.) pp 131–204, Plenum, New York.
Demel, R. A., London, Y., Geurts van Kessel, W. S. M., Vossenberg, F. G. A., & van Deenen, L. L. M. (1973) *Biochim. Biophys. Acta 311*, 507–519.
Demel, R. A., Geurts van Kessel, W. S. M., Zwaal, R. F. A., Roelofsen, B., & van Deenen, L. L. M. (1975) *Biochim. Biophys. Acta 406*, 97–107.
Demel, R. A., Paltauf, F., & Hauser, H. (1987) *Biochemistry 26*, 8659–8665.
de Vrije, G. J., Tommassen, J., & de Kruijff, B. (1987) *Biochim. Biophys. Acta 900*, 63–72.
de Vrije, G. J., de Swart, R. L., Dowhan, W., Tommassen, J., & de Kruijff, B. (1988) *Nature (London)* (in press).
Dierstein, R., & Wickner, W. (1985) *J. Biol. Chem. 260*, 15919–15924.
DiRienzo, M., Nakamura, K., & Inouye, M. (1978) *Annu. Rev. Biochem. 47*, 481–532.
Dottavio-Martin, D. & Ravel, J. M. (1978) *Anal. Biochem. 87*, 562–565.
Engelmann, D. M., & Steitz, T. A. (1981) *Cell (Cambridge, Mass.) 23*, 411–422.
Fiske, C. H., & Subbarow, Y. (1925) *J. Biol. Chem. 66*, 375–389.
Geller, B. L., & Wickner, W. (1985) *J. Biol. Chem. 260*, 13281–13285.
Hille, J. D. R., Donné-Op den Kelder, G. M., Sauve, P., de Haas, G. H., & Egmond, M. R. (1981) *Biochemistry 20*, 4068–4073.
Inouye, M., & Halegoua, S. (1980) *CRC Crit. Rev. Biochem. 7*, 339–371.
Laxma Reddy, G., & Nagaraj, R. (1985) *Biochim. Biophys. Acta 831*, 340–346.
Meyer, D. I., Krause, E., & Dobberstein, B. (1982) *Nature (London) 297*, 647–650.
Mombers, C., Verkleij, A. J., de Gier, J., & van Deenen, L. L. M. (1979) *Biochim. Biophys. Acta 551*, 271–281.
Müller, M., & Blobel, G. (1984) *Proc. Natl. Acad. Sci. U.S.A. 81*, 7737–7741.
Nagaraj, R. (1984) *FEBS Lett. 165*, 79–82.
Nanba, S., Hikawa, A., Kitoo, N., Horigome, T., Omata, S., & Suganu, H. (1984) *J. Biochem. (Tokyo) 96*, 1133–1142.
Nesmeyanova, M. A. (1982) *FEBS Lett. 142*, 189–193.
Oliver, D. B., & Beckwith, J. (1981) *Cell (Cambridge, Mass.) 25*, 765–772.
Ohno Iwashita, Y., & Wickner, W. (1983) *J. Biol. Chem. 258*, 1895–1900.
Perlman, D., & Halvorson, H. O. (1983) *J. Mol. Biol. 167*, 391–409.
Pilon, M., Jordi, W., de Kruijff, B., & Demel, R. A. (1987) *Biochim. Biophys. Acta 902*, 207–216.
Rietveld, A., Ponjee, G. A. E., Schiffers, P., Jordi, W., van de Coolwijk, P. J. F. M., Demel, R. A., Marsh, D., & de Kruijff, B. (1985) *Biochim. Biophys. Acta 818*, 398–409.
Rietveld, A., Jordi, W., & de Kruijff, B. (1986) *J. Biol. Chem. 261*, 3846–3856.
Rosenblatt, M., Beaudette, N. V., & Fasman, G. D. (1980) *Proc. Natl. Acad. Sci. U.S.A. 77*, 3983–3987.
Rouser, G., Fleischer, S., & Yamamoto, A. (1975) *Lipids 5*, 494–496.
Schindler, H. (1979) *Biochim. Biophys. Acta 555*, 316–336.
Seelig, J. (1978) *Biochim. Biophys. Acta 515*, 105–140.
Shah, D. O., & Schulman, G. (1965) *J. Lipid Res. 6*, 341–346.
Shiba, K., Ito, K., Yura, T., & Cerretti, D. P. (1984) *EMBO J. 3*, 631–635.
Shinnar, A. E., & Kaiser, E. T. (1984) *J. Am. Chem. Soc. 106*, 5006–5007.
Singer, S. J., Maher, P. A., & Yaffe, M. P. (1987) *Proc. Natl. Acad. Sci. U.S.A. 84*, 1015–1019.
Sjöström, M., Wald, S., Wieslander, Å., & Rilfors, L. (1987) *EMBO J. 6*, 823–831.
Smaal, E. B., Romijn, D., Geurts van Kessel, W. S. M., de Kruijff, B., & de Gier, J. (1985) *J. Lipid Res. 26*, 633–637.
Steiner, D. F., Quinn, P. S., Chan, B. J., Marsh, J., & Tager, H. S. (1980) *Ann. N.Y. Acad. Sci. 343*, 1–16.
Tamm, L. K. (1986) *Biochemistry 25*, 7470–7476.
van Deenen, L. L. M., & de Haas, G. H. (1964) *Adv. Lipid Res. 2*, 168–229.
van Dijck, P. W. M., de Kruijff, B., van Deenen, L. L. M., de Gier, J., & Demel, R. A. (1976) *Biochim. Biophys. Acta 455*, 576–587.
Vogel, H., & Jähnig, F. (1986) *Biophys. J. 50*, 573–582.
von Heijne, G. (1984) *EMBO J. 3*, 2315–2318.
von Heijne, G. (1985) *J. Mol. Biol. 184*, 99–105.
von Heijne, G., & Blomberg, C. (1979) *Eur. J. Biochem. 97*, 175–181.
Walter, P., & Blobel, G. (1980) *Proc. Natl. Acad. Sci. U.S.A. 77*, 7112–7116.
Wiech, H., Sagstetter, M., Muller, G., & Zimmermann, R. (1987) *EMBO J. 6*, 1011–1016.
Wiedmann, M., Kurzchalia, T. V., Hartmann, E., & Rapoport, T. A. (1987) *Nature (London) 328*, 830–833.
Yatvin, M. B. (1987) *Biochim. Biophys. Acta 901*, 147–156.